2017

A Packaged Whispering Gallery Mode Strain Sensor Based on a Polymer Wire Cylindrical Micro Resonator

Vishnu Kavungal
Technological University Dublin, vishnu.kavungal@tudublin.ie

Gerald Farrell
Technological University Dublin, gerald.farrell@tudublin.ie

Qiang wu
Technological University Dublin, qiang.wu@tudublin.ie

See next page for additional authors

Recommended Citation

Kavungal, V., Farrell, G. & Wu, Q. (2017). A Packaged Whispering Gallery Mode Strain Sensor Based on a Polymer Wire Cylindrical Micro Resonator. *Journal of Lightwave Technology*, vol. PP, no. 99. doi:10.1109/JLT.2017.2784678

A packaged whispering gallery mode strain sensor based on a polymer-wire cylindrical micro resonator

Vishnu Kavungal, Gerald Farrell, Qiang Wu, Arun Kumar Mallik, and Yuliya Semenova

***Abstract*— We propose a whispering gallery mode (WGM) strain sensor formed by a polymer-wire cylindrical micro resonator for strain measurement applications. WGMs are generated by evanescently coupling light into the polymer-wire resonator from a silica fiber taper fabricated by the micro heater brushing technique. Accurate and repeatable measurements of a strains up to one free spectral range (FSR) shift of the WGMs (corresponding to 0.33 % of the polymer-wire elongation, 3250 με) are demonstrated experimentally with the proposed sensor. Practical packaging method for the proposed strain sensor on a glass microscope slide has also been realized making the sensor portable and easy to handle. The robustness of the packaged coupling system is confirmed by vibration tests. The performance of the packaged strain sensor is evaluated and compared with that for an unpackaged sensor.**

***Index Terms*—Whispering gallery modes, Optical fiber sensors, Optoelectronic and photonic sensors, Mechanical sensors, Microsensors, Force sensors, Cavity resonators, Resonator filters, Optical tuning.**

I. INTRODUCTION

STRAIN is a measure of the deformation of an object when subject to an applied force. Specifically, it is the fractional change in dimension (length, width, or height) when subject to a force along that dimension. In a traditional strain gauge, stretching causes a change in the resistance of the metal grid whose value can be related to the value of applied strain. The operation of optical fiber strain sensors is based on measurements of light transmission or wavelength shift resulting from changes in the shape as well as the optical properties of the fiber materials due to the applied strain. The unique advantages of optical fiber strain sensors are high signal-to-noise ratio, light weight, small size, ease of installation, and immunity to electromagnetic interference. Optical fiber strain sensors are intrinsically passive and can be safely utilised in high voltage and potentially explosive environments [1].

However, silica fiber based strain sensors have a limited sensitivity and possess a tensile strain range only up to 4000 με (limited by the breakage strain threshold corresponding to 0.4% fiber elongation) [2, 3] because of the relatively high elastic modulus of silica. Strain sensitivity can be improved by using fiber materials with a smaller elastic modulus such as polymers. Furthermore, flexibility and deformability of the polymer materials makes them capable of surviving larger applied strains without breakage compared to silica. There are many reports on fiber optic strain sensors employing single mode and multimode polymer optical fibers (POFs) as strain sensors including FBGs written in conventional and micro-structured POF [3, 4]. A POF multimode interference sensor has also been reported [5]. It should be noted however, that the polymer sensor types above require substantial effort in terms of fabrication and cost (for example FBG writing, photomasks, fiber hetero-structure fabrication, depending on the sensor type).

For over a decade whispering gallery mode (WGM) optical micro-resonators (MRs) have received a lot of attention for application as various forms of sensor because of their high-quality factors and low mode volume [6, 7]. There are many reports concerning WGM strain sensing using spherical [8-14] as well as bubble [15, 16] MRs based on silica and polymer materials. Typically, an evanescent light coupling technique is used to excite the WGMs in such MRs. This involves placing the MR in physical contact with a thin and often fragile fiber taper. The practical application of such spherical or bubble-shaped MRs for strain sensing is limited due to the need to maintain the precise alignment between the resonator and the fiber taper for optimal and stable coupling, independent of external vibrations. Practical applications are also hindered by the absence of a suitable packaging technique which would allow the sensor to reliably sense strain whilst maintaining long term alignment of the sensor elements. One approach to reducing the difficulty of maintaining alignment accuracy is to utilise MRs with a cylindrical shape, since such an MR-taper structure has only one degree of freedom compared to two degrees of freedom for the case of spherical symmetry [17].

Recently we reported a study of a strain-induced spectral

This work was supported by Dublin institute of technology under Fiosraigh scholarship program. (*Corresponding author: Vishnu Kavungal*)

Vishnu Kavungal, Gerald Farrell, Arun Kumar Mallik, and Yuliya Semenova with Photonics research center, Dublin institute of technology, Kevin street, Dublin 8, Ireland (e-mail: vishnu.kavungal@mydit.ie; gerald.farrell@dit.ie; d13125763@mydit.ie; yuliya.semenova@dit.ie)

Qiang Wu was with Photonics research center, Dublin institute of technology, Kevin street, Dublin 8, Ireland. He is now with Department of mathematics, Physics, and Electrical engineering, Northumbria university, Newcastle upon Tyne, NE1 8ST, United Kingdom. (e-mail: qiang.wu@northumbria.ac.uk).

tunability of WGMs excited in a coating-stripped POF cylindrical MR [18], fabricated from a short section of commercially available POF with the outer diameter of 490 μm. That study demonstrated that such resonators are potentially very suitable as highly sensitive strain sensors due to the good stability and repeatability of their performance and also due to the excellent elastic properties of the polymer materials, leading to a large dynamic range for strain sensing.

In this paper, we report the development and experimental demonstration of a practical packaged strain sensor based on the strain tunability of WMGs in a polymer cylindrical resonator. To avail of greater flexibility in terms of cylindrical MR sizes, in this work we replaced a commercial POF (available only in a few standard diameters) with a laboratory drown wire made from a polymethyl-methacrylate (PMMA) rod as a cylindrical MR for strain sensing. It should be noted, that fabrication of such a wire is significantly simpler in comparison with the commercial POF drawing process, since the MR does not require formation of the fiber core. Similar to the previous work [18], the WGMs in the MR were evanescently excited using a tapered silica optical fiber. In the following sections of this paper, we present the results of the characterization of the strain sensor performance. Furthermore, the packaging of the proposed sensor is demonstrated based on a glass slide acting as a substrate, which results in a portable and easy to handle sensor. The entire proposed packaging process is also simple and takes less than 10 minutes to complete. After the packaging, the robustness of the strain sensing micro-resonator and tapered fiber coupling system is confirmed by vibration tests. Finally, the influence of input light polarization on the light coupling efficiency is investigated and presented. To the best of our knowledge this work is a first comprehensive demonstration of a packaged WGM cylindrical strain sensor formed by a polymer wire cylindrical micro resonator packaged on a glass substrate. Our proposed method offers higher strain sensitivity compared to similar sensors based on silica fibers, and in addition offers higher mechanical stability (compared with spherical, bottle, and bubble microresonators) making it a suitable candidate for strain/stress and displacement sensing, especially in applications where a small sensor footprint is required.

II. Sensing principle, operation and fabrication

The operating principle of the sensor is based on the measurement of the spectral shift of WGM resonances excited in the cylindrical MR as a result of changes in its diameter due to the applied axial strain or stress. The resonance condition for the light circulating within the MR is fulfilled if the light wave reaches the point of its origin with the same phase after traveling one full circle of the resonator. The resonant wavelengths for which the resonance condition is satisfied are "trapped" within the resonator resulting in the appearance of the spectral dips in the transmission spectrum of the coupled fiber taper. Typically, WGM resonances excited in a fiber cylindrical MR have Q-factors in the order of ~ 10^4. Under the influence of the axial strain or stress applied to the MR, both its diameter and the effective refractive index of its material change, resulting in a spectral shift of the WGM resonances.

In our experiment, we used a short section of a polymer wire as the strain sensing MR. The polymer wire was fabricated by heating and stretching of a polymethyl methacrylate (PMMA) rod to a diameter of 230 μm at a temperature of 180°C.

For the fabrication of the tapered fiber, a short length of a coating-stripped standard single mode telecommunication optical fiber (SMF 28, Coring) with core and cladding diameters of 8.3 μm, and 125 μm respectively was stripped of its coating and cleaned with isopropyl alcohol. The coating-stripped section then was fixed horizontally between two computer controlled XYZ translational stages. The tapered fiber was then fabricated by means of the customized micro-heater brushing technique described in [20]. A ceramic micro heater (CMH-7019, NTT-AT) was used to heat the fiber up to approximately 1300°C, making the silica material soft enough for tapering. A customized PC program allowed for an accurate control of the diameter, the length, and the shape of the fabricated tapers. In our experiment the fabricated tapered fiber waist diameter is approximately 1.3 μm, the waist length is around 6 mm and the full taper length is circa 50 mm.

A 40 mm length of the polymer wire resonator was fixed with one of its ends clamped to a holder and the other end connected to a micro-translation stage with 10 μm movement resolution. Broadband light from a super luminescent diode (SLD) was launched into the fabricated tapered single mode silica optical fiber, which was placed in contact with the polymer MR similarly to the setup described in [18], and the resulting WGM spectrum was recorded at the output of the taper using an optical spectrum analyzer (OSA) with a 10 pm spectral resolution.

Figure 1 (a) & (b) show the transmission spectrum of the tapered fiber of waist diameter 1.3 μm coupled with a cylindrical polymer wire resonator with the diameter of 230 μm. Periodic narrow resonance peaks with a quality factor of circa ~ 10^3 and average free spectral range (FSR) of 2.35 nm are observed in the wavelength range from 1500 to 1520 nm. The maximum extinction ratio for the resonant dips reaches 23 dB. The relatively high transmission loss of the spectrum is due to the high optical absorption by the polymer material in the infrared region, coupling losses, scattering losses on residual surface inhomogeneities, losses introduced by surface contaminants and the slight microbend loss arising in the thin microfiber due to its contact with a relatively thicker cylindrical resonator [19, 20].

To characterize the strain sensing performance of the setup, strain was applied to the polymer wire resonator axially by moving the translation stage with a step of 10 μm (corresponding to an axial strain of 250 με (0.03% fiber elongation)) in a direction away from the fixed end. During each measurement of the shift of the WGM spectrum with respect to the applied strain, the input polarization state was remained unchanged. All the measurements were carried out at a constant laboratory temperature (20 °C).

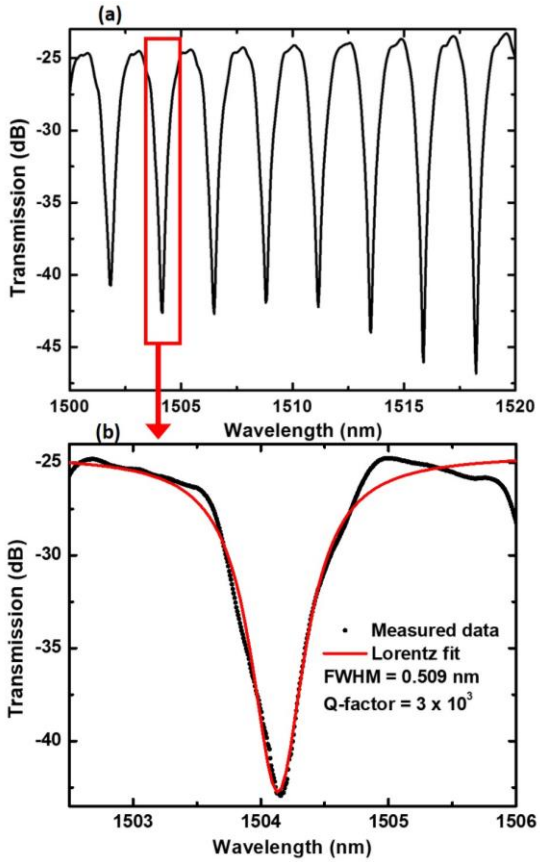

Figure 1. (a) Transmission spectrum of tapered fiber coupled with a 230 μm diameter cylindrical polymer wire resonator. (b) Selected single resonance dip along with the Lorentzian fit.

Figure 2 illustrates the effect of axial strain on the selected WGM dip (1518.2 nm at zero strain) in the transmission spectrum. As the axial strain increases from zero to 3250 με (0.33% polymer-wire elongation), the resonant dip exhibits a progressively larger blue shift close to the FSR range (2.33 nm). As can be seen from the figure, the selected WGM resonance shifts towards shorter wavelengths with the increase of applied strain. It should be noted that at high tensile strains (> 1250 με), additional side-lobes appear in the selected WGM spectra, possibly due to strain-induced deformations and deviation of the resonator from its cylindrical shape [21].

A 40-mm long polymer-wire used in the experiment is capable of sustaining an axial elongation of 3 to 3.5 mm (corresponding tensile strain is 7.5 – 8.8 × 10^4 με). In the polymer-wire resonator-tapered fiber coupling arrangement, a 6% of its axial elongation (corresponding tensile strain is 6 × 10^4 με) can be applied by without the need of fiber taper realigning. Beyond this estimated strain value, by continuing the elongation, the chance of breakage of the polymer-wire is increased and WGMs coupling efficiency is significantly degraded.

As demonstrated by Klitzing *et al.* [22], designing a useful device for a specific strain sensing application it is desirable to limit the range of the applied strains so that the corresponding WGMs spectral shift occurs within the FSR range of the spectrum in order to avoid ambiguities in identifying the position of a strained modes with respect to the unstrained modes. It is also important to avoid changes in modal components order due to strain induced deformations of the polymer wire. Therefore, in our experiments the strain range is limited so that WGMs shift is less than one FSR corresponding to 0.33% (3250 με) axial elongation of the polymer wire.

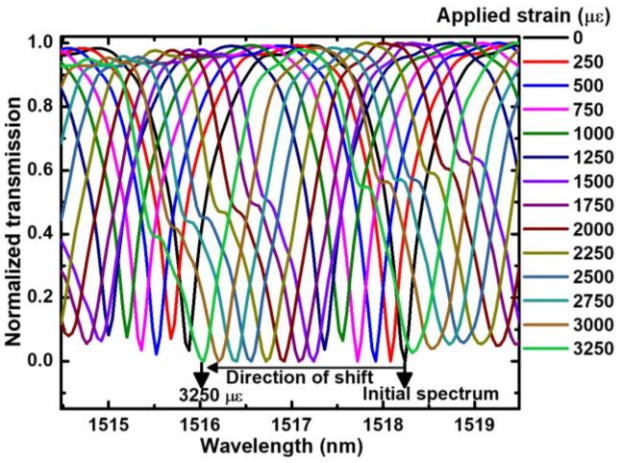

Figure 2. Shift in the selected dip of WGM transmission spectrum with increasing axial strain.

The spectral shift of the WGM resonant wavelength due to axial strain can be described as a combined effect of changing diameter and the changing refractive index of the resonator [8-15, 23]:

$$\frac{\Delta\lambda}{\lambda} = \frac{\Delta D}{D} + \frac{\Delta n}{n} \tag{1}$$

where $\Delta D/D$ is the fractional change in the MR diameter (D) due to the deformation of the micro-cavity and $\Delta n/n$ is the fractional change in the refractive index (n) due to the strain-optic effect. The transverse deformation ($\Delta D/D$) of the micro- cavity can be related to the axially applied tensile strain ($\Delta L/L$) by the Poisson ratio (σ). The Poisson ratio, is the ratio of the lateral contraction strain ($\Delta D/D$) to the axial tensile strain ($\Delta L/L$) given by:

$$\sigma = \frac{\Delta D / D}{\Delta L / L}. \tag{2}$$

Changes in the fiber dimensions result in changes in the material density with the corresponding induced changes in its refractive index (Δn). Thus, changes in the refractive index can be expressed as

$$\Delta n = n P_{eff} \frac{\Delta L}{L} \tag{3}$$

where P_{eff} is the effective strain-optic coefficient [5, 18, 20]. The total WGM resonance wavelength shift can be expressed as

$$\frac{\Delta\lambda}{\lambda} = -\left(\sigma \frac{\Delta L}{L} + P_{eff} \frac{\Delta L}{L}\right) \tag{4}$$

Here the negative sign shows that the axial tensile strain applied to the POF micro-resonator will result in a blue shift of

the WGM resonance. The Poisson's ratio and the effective strain-optic coefficient of PMMA are 0.35-0.45 and 0.099 (±0.0009) respectively [5, 18, 23, 25].

Figure 3 shows the Theoretically calculated and experimentally measured wavelength shift as a function of axial strain for a selected WGM dip. Here the solid red line is the strain dependence of WGM wavelength shift calculated using equation (4) by setting the Poisson's ratio (σ) of the PMMA wire resonator to 0.35, and the resonance wavelength to 1550 nm. The slope of the calculated linear dependence indicates a theoretical strain sensitivity of -0.69 pm/με. The theoretically calculated total shift of the WGMs in response to strain associated with a 0.33 % polymer wire elongation is 2.26 nm.

The scattered data in figure 3 shows the experimentally measured wavelength shift for a selected WGM dip versus the applied strain. The slope of the linear dependency of the measured data is calculated as -0.68 pm/με, which agrees well with the theoretically calculated value. There is an average 0.2 nm blue shift for the WGMs dip for each 10 μm elongation (250 με). From the experimental results one can see that the resonance wavelength shift is quite in line with the theoretically calculated shift thus the proposed system offers good potential as a strain sensor. The total shift of WGMs is 2.2 nm in response to the 0.33% strain, which agrees with the theoretically calculated shift.

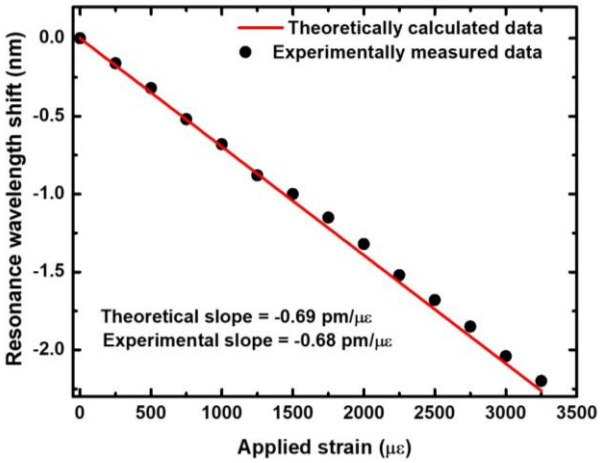

Figure 3. Theoretically calculated and experimentally measured wavelength shift as a function of axial strain for a selected WGM dip.

III. Strain Sensor Packaging Experiment

In laboratory conditions, evanescent coupling of light from a fiber taper into a spherical, bottle or bubble MR is typically realized by means of high-resolution 3D micro-positioning stages and optical microscopes, to permit precise alignment of the tapered fiber waist region along the MR equator at a close distance to the resonator surface. As mentioned above, evanescent light coupling to a cylindrical micro resonator is somewhat simpler since only 2D alignment is necessary. However, in real world applications even the least complex scenario becomes impractical if it demands bulky and heavy micro-positioning equipment as an integral part of the system. Therefore, for practical applications the development of a simple and reliable packaging method is required for WGM based sensors which allows precise alignment of the sensor elements to be initially achieved using micro-positioning equipment but then ensures that precise alignment can be maintained without the continued use of the micro-positioning equipment. This in turn enables the fabrication of portable and miniature devices without degrading their laboratory performance.

Recently Ilchenko *et al.* reported the realization of a compact packaged narrow-linewidth laser based on a WGM resonator with a prism coupler [26]. Yan *et al.* [27] and Wang *et al.* [28] demonstrated a packaging method for a tapered fiber-coupled spherical micro resonator utilizing low refractive index UV curable glue as the coating material. The authors also carried out temperature and photosensitivity studies to evaluate the device performance after packaging. More recently Dong *et al.* proposed a packaging technique for spherical [29], and cylindrical [30] microresonators coupled with a tapered fiber. In their packaging technique, the resonator rested on the thin portion of the tapered optical fiber like a cantilever to achieve light coupling and generate WGMs, utilizing the force of gravity instead of glue. The same authors also confirmed the robustness of the coupling system by a vibration test. A special kind of packaging for a tapered fiber-microsphere system was demonstrated by K. Milenko et al. [29], where a silver iodide metaphosphate glass microsphere was thermally melted and attached on to a tapered optical fiber. Temperature characterization of the packaged device was also performed.

In this work, we propose and demonstrate a packaging method based on three simple steps which involves gluing the resonator and the light coupling tapered fiber on to glass substrate. The robustness of the coupling system is confirmed by testing the packaged device under strong vibration conditions.

The proposed packaging process can be completed in three steps: (a) preparation of the tapered fiber and polymer wire resonator arrangement, (b) maximizing the coupling efficiency between the tapered optical fiber and the polymer wire resonator and (c) immobilizing the coupled system on a glass substrate using UV curable epoxy.

A. Preparation of the polymer wire resonator for coupling

In order to prepare the polymer micro-cylinder for packaging, a short section of silica capillary tube was attached on to a glass substrate using UV- curable glue (Loctite AA 358) as shown in Figure 4 (1). Then a flexible polymer wire with a uniform outer diameter of 230 μm was inserted into the attached silica capillary tubing as illustrated in Figure 4 (2). The capillary tube's inner diameter must be slightly larger than the polymer wire's outer diameter. In the last step, shown in Figure 4 (3), one end of the polymer wire was attached on to the glass substrate using UV- curable glue. The capillary tube has a significant role in the packaging process as it allows attachment of the polymer wire resonator to the glass substrate while ensuring free axial movement of the polymer wire due to applied strain. The total length of the polymer wire in our

experiment was 80 mm. The inner diameter and the length of the capillary tubing were circa 240 μm and 5 mm respectively. To achieve a tighter fit between the inner diameter of the tubing and the outer diameter of the polymer wire resonator, the silica tubing's diameter may be reduced by tapering using the same technique used for fabrication of the tapered fiber.

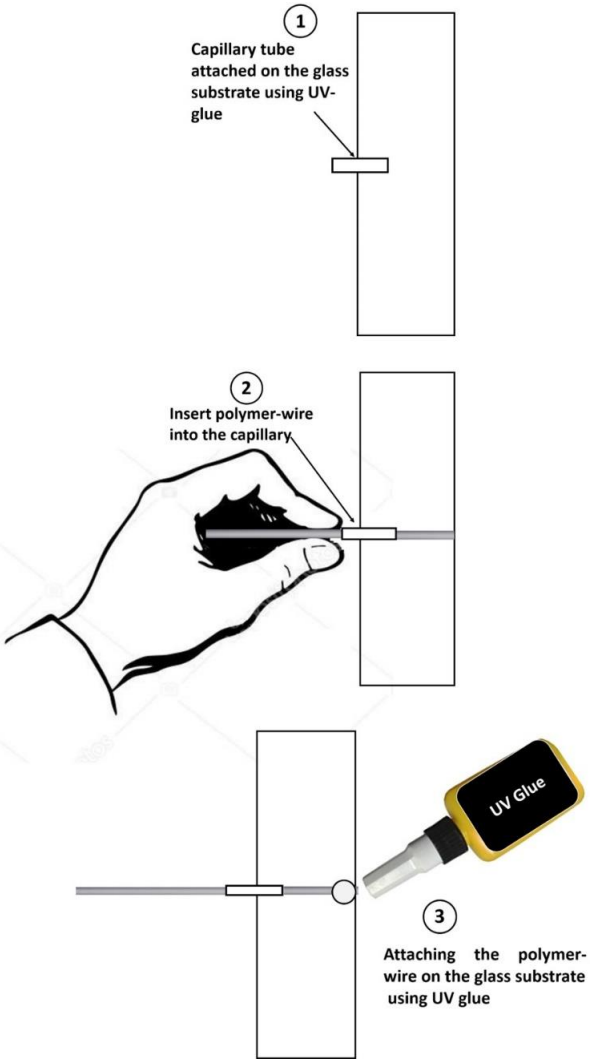

Figure 4. Schematic of the packaging process: (1) Capillary tube attached on the glass substrate, (2) inserting polymer-wire into the capillary tube, and (3) attaching the polymer wire on to the glass substrate using UV glue.

B. Maximizing the coupling efficiency

The presence of large evanescent field outside of the tapered portion of the fiber makes it possible to couple the light into the strain sensing polymer wire acting as the micro-cylinder by placing both in direct physical contact.

Figure 5 (a) illustrates schematically the experimental setup for optimizing the coupling efficiency between the tapered optical fiber and the polymer wire sensor probe. The prepared strain sensing polymer wire resonator shown in Figure 4 (3) is fixed on a translation stage with an adjustable 3D- positioner. Using the vertical positioner, the polymer wire was brought in contact with the tapered fiber to excite the WGMs. It should be noted that due to the difficulty of manipulating the thin and fragile tapered silica fiber, this step was carried out while the fiber taper was still secured horizontally between the two translational stages of the taper-drawing setup after its fabrication.

This process of micro-alignment is assisted by a fiber coupled He-Ne laser radiating at 632.8 nm, connected to the input of the tapered fiber. The leaked red light made the taper waist region clearly visible and helped to align it perpendicularly with the polymer wire resonator. When the alignment process was completed, the He-Ne laser at the input end of the fiber taper was replaced with a super luminescent diode (SLD) (Thorlabs), with a wavelength range of 1500-1600 nm and the output of the fiber taper was connected to the OSA (86142B, Agilent).

After achieving the physical contact with the tapered fiber, the polymer wire was slowly moved along the taper axis while maintaining physical contact and mutually orthogonal orientation. During this operation, the transmission spectrum of the taper was observed at the OSA screen to determine the optimal position of the contact point, corresponding to the phase match between the propagating mode of the fiber taper and the fundamental WGM of the polymer wire resonator [32].

C. Immobilizing the coupled system on a glass substrate

After achieving the desired WGM spectrum quality, vis-à-vis a high extinction ratio and Q-factor, the tapered fiber was glued to the glass slide using UV curable epoxy. Before applying the glue, the physical contact between the fiber taper and the polymer wire was ensured using spacers with an appropriate thickness attached to the glass substrate serving as the basis for the coupling arrangement. The entire packaging process took less than 10 minutes.

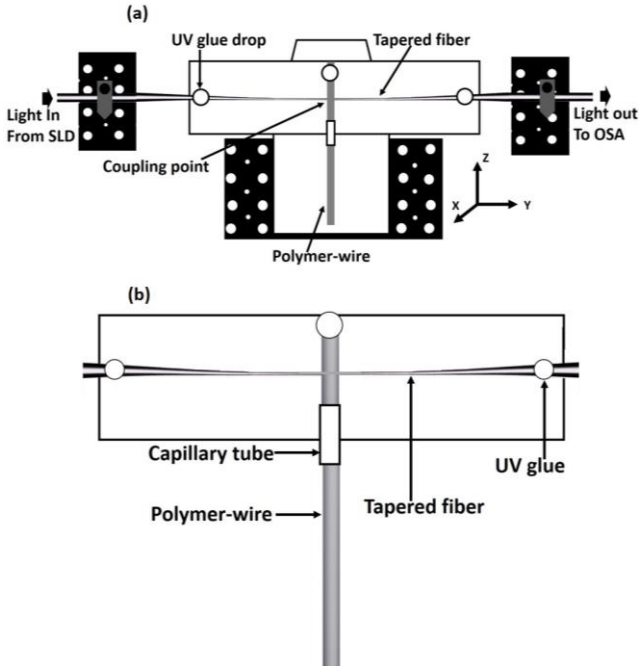

Figure 5. (a)-(b) Illustration of the packaging process

Figure 5 (b) shows the schematic diagram of a packaged strain sensor. The photograph of the packaged strain sensor is shown in Figure 6.

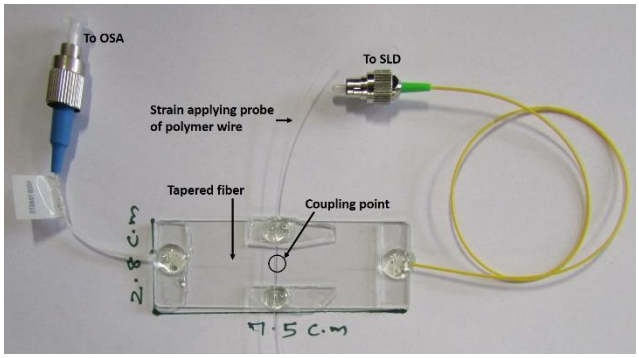

Figure 6. Photograph of the packaged strain sensor.

D. Before/after packaging performance comparison

Figures 7 (a, b) show the transmission spectra of the tapered fiber before and after the packaging. Narrow resonances with a Q-factor in the order of ~ 10^3 were observed in both spectra. There is a change in the extinction ratio of the WGM spectrum before and after packaging also accompanied by a small spectral shift in the order of picometer. This is possibly due to the increased coupling loss and changing polarization of the input light.

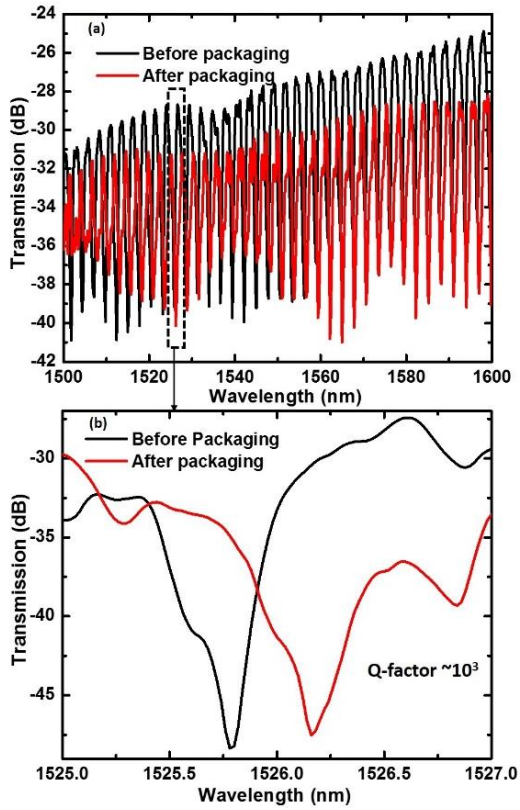

Figure 7. (a) Transmission spectrum of the tapered fiber before and after packaging (b) selected single resonance dip.

IV. Analysis of the Performance of the Packaged Strain Sensor

To evaluate the performance of the packaged device, strain sensing experiments were carried out at a constant laboratory temperature (20 °C). Figure 8 illustrates the experimental setup used for characterization of the packaged WGM based strain sensor. Similar to the previous experiments, one end of the tapered fiber is connected to the SLD through a three-paddle polarization controller and the output end is connected to an OSA with a 10 pm resolution. The packaged strain sensor is clamped onto an optical platform. The free end of the polymer wire is fixed on a micro translation stage with a 10 μm movement resolution. The distance between the two fixed points (A and B) of the polymer wire is considered as the sensing length. Here the sensing length was set to 40 mm for consistency.

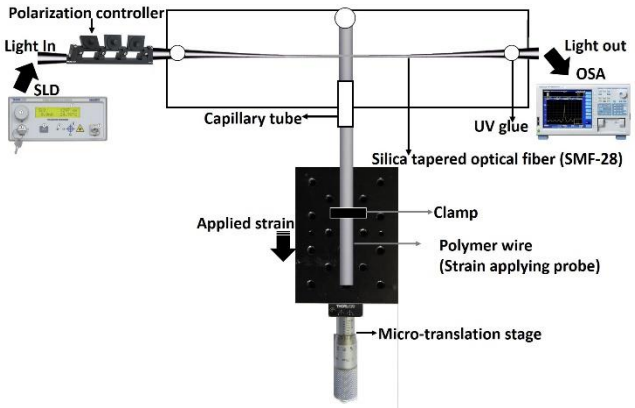

Figure 8. Schematic diagram of the strain sensing experiments using the packaged strain sensor.

Strain is applied to the polymer wire by moving the translation stage with a step of 10 μm (corresponding to an axial tensile strain of 250 με) in a direction away from the fixed end. Figures 9 (a) show the spectral shift experienced by a selected WGM dip as the axial strain is increased from zero to 2500 με. Similar to the previous experiments, when the axial strain increases, the resonant dips exhibit a linear blue shift. For testing the repeatability of the packaged sensor performance, we carried out a reversed cycle of measurements where the applied axial strain was decreased back to zero, during which the resonance dips linearly red-shifted back to their initial positions with a relatively low level of hysteresis. Figure 9 (b) shows the resonance wavelength shift with the decreasing applied strain and Figure 9 (c) illustrates the hysteresis between the two opposite cycles, where the bottom axis represents the increasing strain and the top axis represents a gradual decrease of the applied axial strain from its maximum value to the initial unstrained state. The maximum difference between the shifted resonance wavelength in the unstrained position is 0.15 nm.

It should be noted that in the case of the packaged sensor, the slope of the linear fit is less than that of the unpackaged sensor, indicating a lower sensitivity to strain (-0.54 pm/με). This is possibly due to the decrease in the efficiency of strain transfer

to the polymer wire induced by the frictional forces from the capillary tube. In the packaged sensor, strain sensitivity can be improved by using more flexible capillary tube as holder.

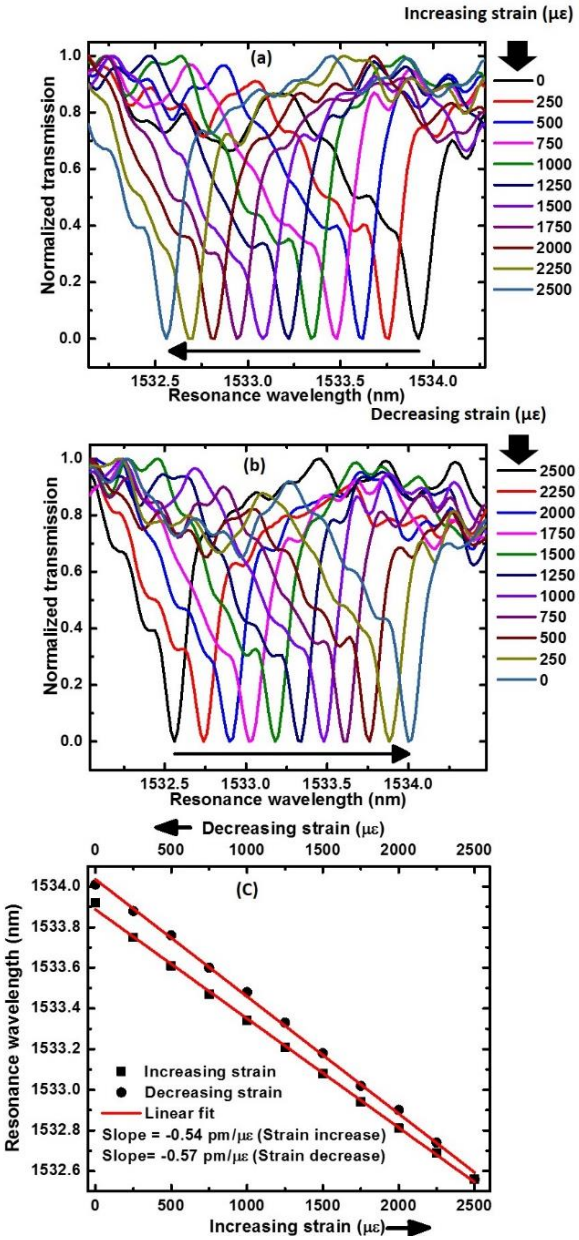

Figure 9. Experimental results for the packaged sensor: (a) & (b) wavelength shift of a selected WGM resonance versus applied increasing (decreasing) strain and (c) & (d) corresponding WGM resonance shifts versus applied strain.

V. STUDIES OF FACTORS AFFECTING THE PERFORMANCE OF PACKAGED SENSOR

A. Mechanical stability

The robustness of the packaged device is evaluated by observing the effect on the transmission spectrum of strong vibrations. For this test, the packaged sensor is placed on the vibration platform (shown in Figure 10) operated with a function generator which can produce various frequency vibrations. A single WGM resonance dip in the transmission spectrum before vibration and after the vibration is shown in Figure 11. One can see from the figure that this resonance dip with a central wavelength of 1526.8 nm does not experience significant changes as a result of vibration. There is a slight decrease in the extinction ratio after the application of vibration but the shape and the Q- factor (~ 10^3) of the resonance dip remain almost constant, indicating that the packaged sensor possesses good resistance to vibration.

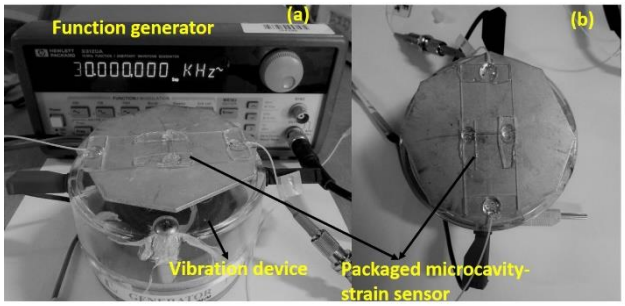

Figure 10. Experimental setup for vibration tests (a) General view; (b) Top view of the vibrational platform.

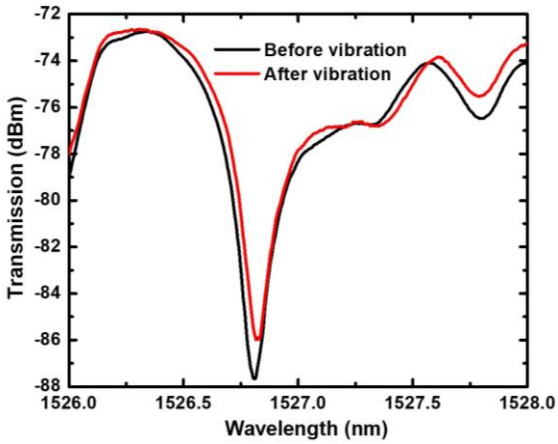

Figure 11. Selected single transmission WGM dip of the packaged strain sensor at before and after vibration.

B. Temperature stability

Temperature sensitivity is an issue for all optical fiber sensors operating in an environment with a varying temperature. The thermal drift of a resonant wavelength in an optical microresonator results from thermal expansion and thermo-optic effects of its material. Fused silica has positive thermal expansion and thermo-optic coefficients. As a result, WGM resonances in a silica microresonator shift towards longer wavelengths with an increase in temperature. The reason behind the red shift is that, when the temperature increases, both the diameter and the refractive index of the material also increase.

This leads to the increase in effective optical path for light within the resonator. To accommodate the larger circumference, the WGM resonance will shift to a longer wavelength.

In the case of optical microresonators made from polymers (PMMA, PDMS), calcium fluoride (CaF_2), or athermal glasses that exhibit negative thermo-optical effect, the refractive index of the material decreases with the increase of the temperature reducing the optical circumference. This leads to the resonance wavelengths shift towards the shorter wavelength side of the spectrum [33]. The temperature induced resonance wavelength shift can be determined from the equation [34],

$$\Delta\lambda = \lambda_0\left(\frac{1}{n}\frac{dn}{dT}\Delta T + \frac{1}{D}\frac{dD}{dT}\Delta T\right) \qquad (5)$$

where $\frac{dn}{dT}$ is the thermo-optic coefficient and $\frac{1}{D}\frac{dD}{dT}$ is the thermal expansion coefficient. The negative thermo-optic coefficient of PMMA is 10^{-4} K^{-1}, one order of magnitude higher than the thermo-expansion coefficient, which is equal to 10^{-5} K^{-1} [35].

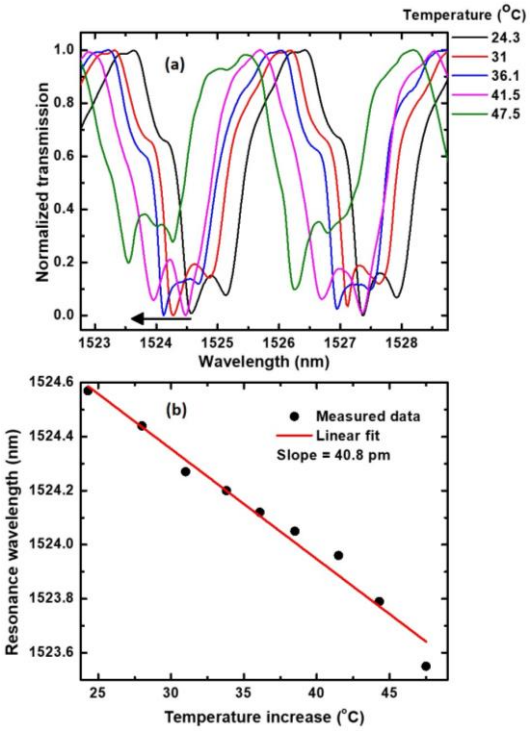

Figure 12. (a) Selected WGM resonance with different applied temperature, and (b) linear fit of the measured resonance wavelength shift data.

To investigate the temperature response of the packaged strain sensor experimentally, sensor's ambient temperature was varied by placing it on a hot stage capable of realizing temperature changes in the range from 20 to 50 °C in 1 °C steps. A reference thermocouple probe with 0.1°C resolution was attached to the surface of the hot stage near the sensor under test. The temperature of the heater then was gradually increased in 2 °C steps and the corresponding changes in the resonance wavelength were recorded using the OSA along with the temperature readings of the thermocouple.

Figure 12 (a) shows the position of a selected WGM resonance at different applied temperatures and Figure 12 (b) analyses the experimental data. Here the scatter data points represent the measured resonance wavelength shifts with increasing temperature and the solid line is a linear fit of the measured data. From the figure one can see that, when the temperature is increased the WGM resonance experiences a blue shift. The slope of the linear fit to the experimental data gives an estimated temperature sensitivity of 40.8 pm/°C. Thus, the estimated temperature cross sensitivity of the strain sensor while operating at increase in temperature conditions is 54 με/°C.

VI. Conclusion

In conclusion, we have proposed a strain sensor based on WGMs excited in a polymer wire cylindrical micro resonator for applications requiring a large dynamic range for strain measurements. The sensitivity of the proposed strain sensor to the increasing axial tensile strain in the range of wavelengths from 1500 to 1600 nm is -0.68 pm/με (unpackaged), and -0.58 pm/ με (packaged) respectively. The light was evanescently coupled into the polymer wire resonator from a standard single mode silica optical fiber taper fabricated by the micro heater brushing technique. Narrow WGM resonances were observed in the fiber taper's transmission spectrum with a Q-factor in the order of 10^3. WGMs are shifted towards shorter wavelengths with increasing axial strain on the resonator. Measurements of axial strains up to 3.25×10^3 με (corresponding to 0.33 % elongation) have been demonstrated, without the need for re-adjustment of the coupling setup due to the impact of applying strain. Furthermore, we proposed and demonstrated a packaging method for the strain sensor on a glass microscope slide which will make the sensor portable and easy to use. The packaging process is simple and robust. Strain sensing experiments were carried out using the packaged sensor at a constant laboratory temperature to demonstrate the sensor performance. The spectral positions of the WGM resonances for the packaged strain sensor shift linearly to shorter wavelengths during the increase in axial tensile strain. The return of WGMs to their original positions with small hysteresis as the decrease of the applied axial strain demonstrates the repeatability of the packaged strain sensor performance. The package sensor was subjected to a range of vibration to determine the sensitivity of the sensor to external vibration. It was found that external vibrations had little or no effect on the sensor performance. The spectral response of the sensor in increasing ambient temperature condition is studied. The estimated temperature cross sensitivity of the strain sensor while operating at increase in temperature conditions is 54 με/°C. The proposed polymer wire based packaged strain sensor possesses several desirable features such as ease of fabrication, small footprint, portability and large dynamic range of strains.

ACKNOWLEDGMENT

Authors would like to acknowledge the support of Dublin Institute of Technology and DIT Fiosraigh Scholarship Program

REFERENCES

[1]. J. M. López-Higuera, Handbook of Optical Fibre Sensing Technology (Wiley, 2002).
[2]. V. Bhatia and A. M. Vengsarkar "Optical fiber long-period grating sensors", *Opt. Lett*. Vol. 21, no. 9, pp. 692-694, 1996.
[3]. H. Y. Liu, G. D. Peng, and P. L. Chu, "Polymer fiber Bragg gratings with 28-dB transmission rejection", *IEEE Photon. Technol. Lett.* Vol. 14, no. 7, pp. 935-937, 2002.
[4]. Y.-J. Rao, Y.-P. Wang, Z.-L. Ran, and T. Zhu, "Novel Fiber-Optic Sensors Based on Long-Period Fiber Gratings Written by High-Frequency CO 2 Laser Pulses" *J. Lightwave Technol*. Vol. 21, no. 5, pp. 1320, 2003.
[5]. J. Huang, X. Lan, H. Wang, L. Yuan, T. Wei, Z. Gao and H. Xiao "Polymer optical fiber for large strain measurement based on multimode interference" *Opt. Lett*. Vol. 37, no. 20, pp. 4308-4310, 2012.
[6]. A. B. Matsko and V. S. Ilchenko, " Optical resonators with whispering gallery modes I: Basics", *IEEE J. Sel. Top. Quantum Electron*, Vol. 12, no. 3, pp. PP3-14, 2006.
[7]. V. S. Ilchenko and A. B. Matsko, " Optical resonators with whispering-gallery modes—Part II: Applications", *IEEE J. Sel. Top. Quantum Electron*, Vol. 12, no. 1, pp. 15-32, 2006.
[8]. V. S. Ilchenko, P. S. Volikov, V. L. Velichansky, F. Treussart, V. Lefevre-Seguin, J, M, Raimond and S. Haroche, "Strain-tunable high-*Q* optical microsphere resonator", *Opt. communications*. Vol. 145, no. 1, pp. 86-90, 1998.
[9]. T. Ioppolo, U. Ayaz1, and M. V. Ötügen, "Tuning of whispering gallery modes of spherical resonators using an external electric field", *Opt. Express*. Vol. 17, no. 19, pp. 16465-16479, 2009.
[10]. T. Ioppolo, M. Kozhevnikov, V. Stepaniuk, M. V. Ötügen, and V. Sheverev, "Micro-optical force sensor concept based on whispering gallery mode resonators", *Appl. Opt*. Vol. 47, no. 16, pp. 3009-3014, 2010.
[11]. T. Ioppolo, U. K. Ayaz, and M. V. Ötügen, "High-resolution force sensors based on morphology dependent optical resonance of polymeric spheres", J. Appl. Phys. 105, 013535-013544 (2009).
[12]. T. Ioppolo, and M. V. Ötügen, "Pressure tuning of whispering gallery mode resonators", *J. Opt. Soc. Am. B*. Vol. 24, no. 1, pp. 2721-2726, 2007.
[13]. U. K Ayaz, T. Ioppolo, and, M. V. Ötügen, "Wall shear stress sensor based on the optical resonances of dielectric microspheres", *Meas. Sci. Technol*. Vol. 22, no. 7, pp. 075203-075212, 2011.
[14]. R. Madugani, Y. Yang, J. M. Ward, J. D. Riordan, S. Coppola, V. Vespini, S. Grilli, A. Finizio, P. Ferraro, and S. Nic Chormaic, "Terahertz tuning of whispering gallery modes in a PDMS stand-alone, stretchable microsphere", *Opt. Lett*. Vol. 37, no. 7, pp. 4762-4764, 2012.
[15]. R. Henze, T. Seifert, J. Ward and O. Benson, "Tuning whispering gallery modes using internal aerostatic pressure", *Opt. Lett*. Vol. 36, no. 23, pp. 4536-4538, 2011.
[16]. M. Sumetsky, Y. Dulashko, and R. S. Windeler, "Super free spectral range tunable optical microbubble resonator", *Opti. Lett*. Vol. 35, no. 11, pp. 1866-1868, 2010.
[17]. G. Farca, S. I. Shopova and A. T. Rosenberger, "Cavity-enhanced laser absorption spectroscopy using microresonator whispering gallery modes", Opt. Express **15**, 17443-17448 (2007).
[18]. V. Kavungal, A. K. Mallik, G. Farrell, Q. Wu, and Y. Semenova, "Strain-induced spectral tuning of the whispering gallery modes in a cylindrical micro-resonator formed by a polymer optical fiber" *Appl. Opt*. Vol. 56, no. 5, pp. 1339-1345, 2017.
[19]. M. Sumetsky, Y. Dulashko, J. M. Fini, A. Hale, and J. W. Nicholson "Probing optical microfiber nonuniformities at nanoscale", *Opti. Lett*. Vol. 31, no. 16, pp. 2393-2395, 2006.
[20]. M. L. Gorodetsky, A. A. Savchenkov, and V. S. Ilchenko, "Ultimate Q of optical microsphere resonators", *Opt. Lett*. Vol. 21, no. 7, pp. 453-455, 1996.
[21]. M. Hossein-Zadeh, and K. J. Vahala, "Fiber-taper coupling to whispering-gallery modes of fluidic resonators embedded in a liquid medium", *Opt. Express*, Vol. 14, no. 22, pp. 10800-10810, 2006.
[22]. W. v. Klitzing, R. Long, V. S. Ilchenko, J. Hare, and V. Lefevre-Seguin, "Frequency tuning of the whispering-gallery modes of silica microspheres for cavity quantum electrodynamics and spectroscopy", *Opt. Lett*. Vol. 26, no. 3, pp. 166-168, 2001.
[23]. C. L. Linslal, M. Kailasnath, S. Mathew, T. K. Nideep, P. Radhakrishnan, V. P. N. Nampoori and C. P. G. Vallabhan, "Tuning whispering gallery lasing modes from polymer fibers under tensile strain" *Opt. Lett*. Vol. 41, no. 3, pp. 551-554, 2016.
[24]. G. Brambilla, V. Finazzi, and D. Richardson, "Ultra-low-loss optical fiber nanotapers," *Opt. Express*. Vol. 12, no. 10, pp. 2258-2263, 2004.

[25]. G. N. Greaves, A. L. Greer, R. S. Lakes and T. Rouxel, "Poisson's ratio and modern materials", Nat. Mat. Vol. 10, no. 11, pp. 823-837, 2011.

[26]. V. Ilchenko, E. Dale, W. Liang, J. Byrd, D. Eliyahu, A. Savchenkov, A. Matsko, D. Seidel, and L. Maleki, "Compact tunable kHz-linewidth semiconductor laser stabilized with a whispering-gallery mode microresonator," *Proc. SPIE* 7913, 79131G (2011).

[27]. Y. Z. Yan, C. L. Zou, S. B. Yan, F. W. Sun, Z. Ji, J. Liu, Y. G. Zhang, L. Wang, C. Y. Xue, W. D. Zhang, Z. F. Han, and J. J. Xiong, "Packaged silica microsphere-taper coupling system for robust thermal sensing application," *Opt. Express* Vol. 19, no. 7, pp. 5753–5759, 2011.

[28]. P. Wang, M. Ding, T. Lee, G. S. Murugan, L. Bo, Y. Semenova, Q. Wu, D. Hewak, G. Brambilla, and G. Farrell, "Packaged chalcogenide microsphere resonator with high Q-factor," *Appl. Phys. Lett*. Vol. 102, no. 7, pp. 13, pp. 131110, 2013.

[29]. Y. Dong, K. Wang, and X. Jin, "Packaged microsphere-taper coupling system with a high Q factor", *J. Appl. Phys*. Vol. 54, no. 2, pp. 277-284, 2015.

[30]. Y. Dong, X. Jin, and K. Wang, "Packaged and robust microcavity device based on a microcylinder-taper coupling system", *J. Appl. Phys*. Vol. 54, no. 13, pp. 4016-4022, 2015.

[31]. K. Milenko, I. Konidakis, and S. Pissadakis, "Silver iodide phosphate glass microsphere resonator integrated on an optical fiber taper", Opt. Lett. Vol. 41, no. 10, 2185-2188, 2016.

[32]. M. Cai, O. Painter, and K. J. Vahala, "Observation of critical coupling in a fiber taper to a silica-microsphere whispering-gallery mode system" *Phys. Rev. Lett*. Vol. 85, no. 1, pp. 74-77, 2000.

[33]. M. Han, and A. Wang, "Temperature compensation of optical microresonators using a surface layer with negative thermo-optic coefficient", *Opt. Lett*. Vol. 32, no. 13, 1800-1802, 2007.

[34]. C. -H. Dong, L. He, Y. -F. Xiao, V. R. Gaddam, S. K. Ozdemir, Z, -F. Hann, G. -C. Guo, and L.Yang, "Fabrication of high-Q polydimethylsiloxane optical microspheres for thermal sensing", Appl. Phy. Lett. Vol. 94, 231119-231122, 2009.

[35]. L. Shi, T. Zhu, D. Huang, and M. Liu, "Thermo–optic tuning of integrated polymethyl Methacrylate sphere whispering gallery mode resonator", *IEEE Photonics Journal*. Vol. 8, no. 5, 2701307 (2016).

Vishnu Kavungal was born in Kerala, India in 1986. He received the B. Sc degree in Physics from Kannur university, Kerala, India, M. Sc degree in Physics and M. Tech degree in optoelectronics & Laser technology from Cochin university of science and technology in 2008 and 2011 respectively. Since May 2013, he has been working toward the PhD degree in Fiber optical sensing from the Photonics research center, Dublin institute of technology, Ireland. His research interest focuses on Optical fiber based whispering gallery mode resonators for sensing application. He is a student member of Optical society of America (OSA), and The Society of Photo-Optical Instrumentation Engineers (SPIE).

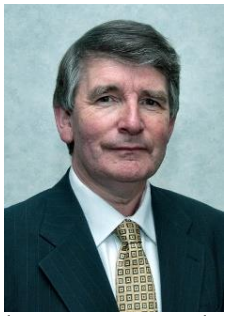

Prof. Gerald Farrell is the founder and Director of the DIT Photonics Research Centre (PRC) at the Dublin Institute of Technology. He leads a multinational research team of researchers focusing on several areas of optical fiber sensing research, for example micro-fiber and nanofiber sensors for chemical and bio-sensing and sensors for composite materials. Prof. Farrell has led several long-term research collaborations with research groups in China, Poland and Australia. He has over 330 publications in the area of photonics and is an Associate Editor and referee for a range of Photonics journals and has been a member of a number of international photonics conference technical committees. He was a Director for several years with the startup company PX Instrument Technology, focusing on the design of optical fiber system test and measurement technologies. He has been involved in a number of research networks, such as the EU COST Action on Optical Sensors and the European Photonics Industry Consortium (EPIC). Prof. Farrell is also a visiting professor in China at Beijing University of Posts and Telecommunications and at Harbin Engineering University. Finally, Professor Farrell is the Dean of the College of Engineering and Built Environment at the Dublin Institute of Technology.

Dr. Qiang Wu is an Associate Professor at Northumbria University, Newcastle Upon Tyne, United Kingdom, He is also an adjunct professor in Beijing University of Posts & Telecommunications and Nanjing University of information Science & Technology. He is a member of editorial board of Scientific Reports and Associate editor of IEEE Sensors Journal. He is a committee member of Holography and Optical information processing committee, The Chinese optical society. His current research interests include fiber optic sensors/biosensors, Nano-fiber, microsphere structure and its application for bio-chemical diagnostics, Nonlinear fiber optics, Optical guided waveguide and surface acoustic wave. He was authored or co-authored over 190 articles in academic journals and international conferences and holds three invention patents.

Arun Kumar Mallik is a Ph.D. student in the photonics research center at the school of electrical and electronics engineering in the Dublin Institute of Technology, Ireland. He will be graduate on December 2017. Previously, He has a M.Tech. Degree in Electronics & communication engineering from Tezpur University, Assam, India in 2007. Between 2007 to 2013 he worked as a researcher at photonics lab in S.A.M.E.E.R (Society for Applied Microwave Electronics Engineering & Research), Mumbai, India. His research interest focuses on Optical fiber based sensors, micro cavity resonators, optical waveguide, femtosecond micro machining, packaging of optical devices.

Prof. Yuliya Semenova is an ME graduate of Lviv Polytechnic National University, Ukraine of 1992. She received her PhD Degree in Physics of Liquid Crystals from the Ukrainian Academy of Sciences in 1999. Between 1997 and 2001 she worked as a researcher at the faculty of Electro-Physics at the Lviv Polytechnic National University. Since 2001 she has been with the School of Electrical and Electronic Engineering at Dublin Institute of Technology. Currently she is a lecturer in the School and principal investigator in the Photonics Research Centre. Her current research interests include liquid crystals, photonics and fiber optic sensing. She has over 270 publications in the area of photonics, many in high impact factor journals. Prof. Semenova is a Vice-Chair of the IEEE Photonics and Electron Devices Society Ireland and a member of the Optical Society of America.